On the coherent components of low-frequency ambient noise in the Indian Ocean

Karim G. Sabra[a)]
School of Mechanical Engineering, Georgia Institute of Technology, Atlanta, Georgia 30332-0405
karim.sabra@me.gatech.edu

Stephanie Fried and W. A. Kuperman
Marine Physical Laboratory, Scripps Institution of Oceanography, La Jolla, California 92037
sefried@mpl.ucsd.edu, wak@mpl.ucsd.edu

Mark Prior
CTBTO Preparatory Commission, Vienna International Centre, P.O. Box 1200, 1400, Vienna, Austria
mark.prior@ctbto.org

Abstract: This letter demonstrates that the dominant coherent component of low-frequency (1 Hz $< f <$ 20 Hz) ambient noise propagating between hydrophone pairs of the same hydroacoustic station, deployed in the deep sound channel of the Indian Ocean, is directional and mainly originates from Antarctica. However, the amplitude of the peak coherent noise arrivals, obtained using a 4-month-long averaging interval, was relatively low given the small hydrophones spacing hydrophones (<2 km). Hence, extracting similar coherent arrivals between two distinct hydroacoustic stations separated instead by thousands of kilometers for noise-based acoustic thermometry purposes seems unlikely, even using a year-long averaging.

PACS numbers: 43.30.Wi, 43.30.Xm, 43.30.Nb [WS]
Date Received: June 22, 2012 **Date Accepted:** November 15, 2012

1. Introduction

As part of the International Monitoring System (IMS) of the Comprehensive Nuclear-Test-Ban Treaty Organization, a network of six underwater hydroacoustic stations has been deployed worldwide [see Fig. 1(a)]. Each IMS hydroacoustic station uses one or two triangular horizontal arrays of three hydrophones, each side of the array being approximately 2 km long. For each array, the three hydrophones are nearly at the same depth within the ocean deep sound channel [or Sound Fixing and Ranging (SOFAR) channel] primarily to allow for long-range detection of man-made (e.g., explosions) or natural (e.g., earthquakes) low-frequency hydroacoustic events (deGroot-Hedlin and Orcutt, 2001; Chapp *et al.*, 2005; Gavrilov and Li, 2009). Furthermore, continuously recording the deep water ocean noise provides a unique opportunity for passive monitoring of the ocean as well as environmental conditions in Antarctica (Gavrilov and Li, 2009; Prior *et al.*, 2011).

Cross-correlation processing of ocean ambient noise has been suggested as a potential means for developing noise-based (or passive) modalities of acoustic ocean monitoring techniques such as acoustic tomography or acoustic thermometry (Roux *et al.*, 2004). This letter demonstrates that coherent arrivals can indeed be extracted

[a)]Author to whom correspondence should be addressed.

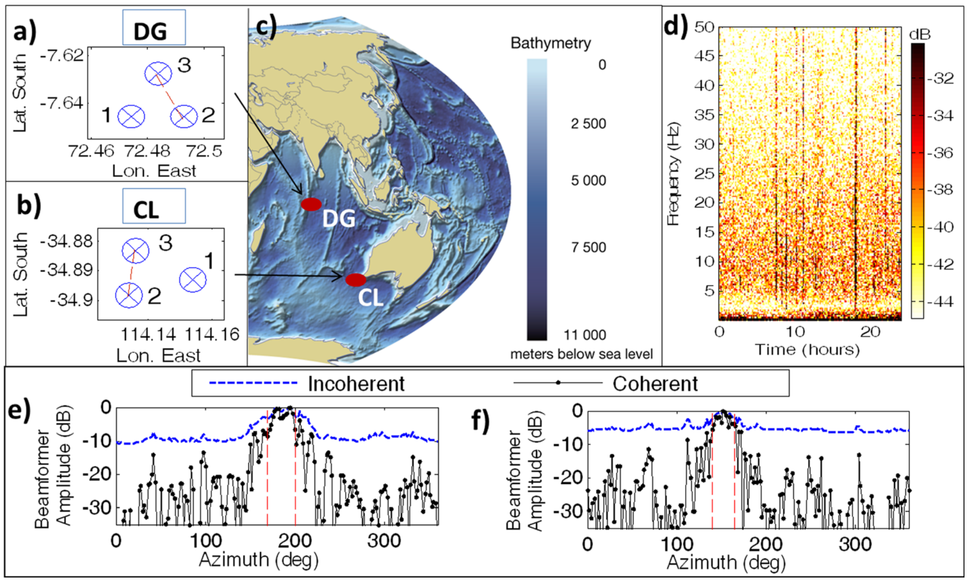

Fig. 1. (Color online) Triangular configuration of the hydroacoustic stations DG (a) and CL (b). (c) Geographic location of DG and CL stations. (d) Spectrogram of the ambient noise recorded on the first hydrophone of the CL station on January 1, 2006. Angular variations of the coherent (plain line) and incoherent (dashed lines) average over 130 days of the plane wave beamformer output (in the frequency band 1–20 Hz) for the hydroacoustic stations CL (e) and DG (f).

from cross correlations of very-low-frequency ocean ambient noise ($1\,\text{Hz} < f < 20\,\text{Hz}$) between pairs of hydrophones of the same hydroacoustic station in deep water. Previous studies of coherent processing of non-episodic ambient noise have typically been conducted at higher frequencies ($f > 50$ Hz), where the ambient noise is usually dominated by (diffuse) shipping noise: Either in the Northern Pacific Ocean of the California coastline (Roux *et al.*, 2004; Godin *et al.*, 2010) or in shallow coastal water (Sabra *et al.*, 2005b; Fried *et al.*, 2008; Siderius *et al.*, 2010; Leroy *et al.*, 2012).

2. Characterization of the ocean ambient noise recorded in the Indian Ocean

For reasons of data availability, this study focuses only on ambient noise recorded during 130 consecutive days (from January 1 to May 10, 2006) recorded by two hydroacoustic stations, labeled DG (Diego Garcia island) and CL (Cape Leeuwin) hereafter, respectively located (1) south of DG and (2) southwest of CL, Australia [see Figs. 1(a)–1(c)]. Ambient noise was recorded continuously. Figure 1(d) displays a typical spectrogram over a 24 h recording period displaying three dominant features, in agreement with previous studies (Gavrilov and Li, 2009; Prior *et al.*, 2011): (1) A very energetic narrowband and continuous component below 0.5 Hz due to ocean microseisms caused by non-linear interactions between waves on the ocean surface; (2) a dominant frequency band of the ocean ambient noise ranging from 1 Hz (corresponding to the lower end of the bandpass filter automatically applied to the stored hydrophone data) up to ~20 Hz; and (3) isolated transient events occurring at random instances (corresponding to vertical lines in the spectrogram). Previous seismic studies have already investigated the use and limitations of ocean miscroseisms for surface wave tomography across ocean basins (Lin *et al.*, 2006). The main interest of this letter is instead the intense very-low-frequency background component ($1\,\text{Hz} < f < 20\,\text{Hz}$) of the ambient noise field that occurred during the 130-day-long analysis window, but not the episodic transient events. Consequently, to reduce the influence of high amplitude transient events while preserving the overall phase information of the time series, the noise recordings were homogenized using the following two processing steps (Sabra *et al.*, 2005a; Fried *et al.*, 2008): (1) Whitening the amplitude spectrum of the data in the band (1–20 Hz) to diminish strong spectral peaks and (2) clipping the signal amplitudes above a threshold equal to three times the average standard deviation of the whitened time series.

Given the frequency whitened and clipped time-series $S_i(t)$ and $S_j(t)$ recorded, respectively, by the ith and jth hydrophones of the selected triangular array ($i,j = 1$–3) during the whole day k ($k = 1$–130), the normalized cross-correlation function $C_{i,j}(t;k)$ for day k is defined by

$$C_{ij}(t;k) = \int_{\mathrm{day}\,k} S_i(\tau) S_j(\tau + t) d\tau \Bigg/ \sqrt{\int_{\mathrm{day}\,k} S_i^2(\tau) d\tau} \Bigg/ \sqrt{\int_{\mathrm{day}\,k} S_j^2(\tau) d\tau}, \tag{1}$$

where t is the time delay (or time lag). The Fourier transform of each cross-correlation function for day k is denoted by $\hat{C}_{ij}(f;k)$ and corresponds to the entry (i,j) of cross-covariance matrix for the selected horizontal triangular array, denoted $\hat{\mathbf{C}}(f;k)$ at the frequency f. The output of the conventional plane-wave beamformer for a given steering azimuth θ can then be computed by (Siderius *et al.*, 2010; Leroy *et al.*, 2012)

$$\hat{B}_k(f,\theta) = W^H(f,\theta)\,\hat{\mathbf{C}}(f;k)\,W(f,\theta), \tag{2}$$

where the symbol H denotes a complex transpose operation and $W(f,\theta)$ is the plane-wave steering vector toward a given azimuth θ (measured clockwise from the north direction). Furthermore, when computing Eq. (2), the diagonal elements $\hat{C}_{ii}(f;k)$ ($i = 1$–3) of the matrix $\hat{\mathbf{C}}(f;k)$ were set to zero to mitigate the bias due to electronic noise and the large incoherent component of the noise field (Westwood, 1992).

Figures 1(e) and 1(f) display the maximum value of the coherent (or incoherent) average over 130 days of the time-domain beamformer $\sum_{k=1}^{130} B_k(t,\theta)$ [or $\sum_{k=1}^{130} |B_k(t,\theta)|$] as a function of the steering azimuth θ. The time-domain beamformer $B_k(t,\theta)$ for the kth day of the 130 day analysis period is the inverse Fourier transform of beamformer $\hat{B}_k(f,\theta)$—see Eq. (2)—across the frequency band (1–20 Hz). The azimuths associated with the mainlobe of the beamformer output—approximately delimited by vertical dashed lines in Figs. 1(e) and 1(f) (155°–210° for CL station and 140°–165° for DG station)—appear to span the section of Antarctica's coastline in the direct line of sight from these two hydroacoustic stations [see Fig. 1(a)]. This spatial origin of the background ocean noise agrees with previous studies which demonstrated that most of the energetic events result from ice-breaking events in the vicinity of Antarctica's coastline, especially during the Austral autumn (i.e., around the month of March) (Chapp *et al.*, 2005; Gavrilov and Li, 2009; Prior *et al.*, 2011).

3. Emergence of coherent arrivals from coherent processing of deep water noise

The averaged cross-correlation waveform $C_{\mathrm{av}}(t;L,N)$ is defined hereafter as the ensemble average of the daily cross-correlations $C_{i=2,j=3}(t;k)$, for hydrophone pair 2–3, between the days L and N of the analysis period ($L \le k \le N$),

$$C_{\mathrm{av}}(t;L,N) = \sum_{k=L}^{N} C_{i=2,j=3}(t;k). \tag{3}$$

This hydrophone pair 2–3 was selected as it points south toward Antarctica's coastline [see the dashed lines in Figs. 1(a) and 1(b)], i.e., toward the dominant origin of the coherent noise field for both the CL array and the DG array [see Fig. 1(c) and Figs. 1(e) and 1(f)]. Figure 2(a) [or Fig. 2(b)] displays the averaged noise cross-correlation waveforms over all 130 days, i.e., $C_{\mathrm{av}}(t;L=1,\ N=130)$ [see Eq. (3)], for both stations CL and DG. Each waveform exhibits a clear coherent arrival (for negative time delay

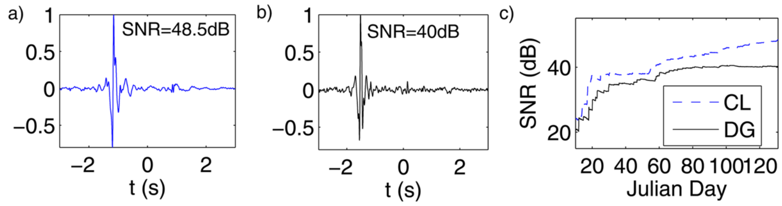

Fig. 2. (Color online) Averaged cross-correlation waveforms $C_{\rm av}(t, L = 1; N = 130)$ [see Eqs. (1) and (3)] between hydrophones 2 and 3 (see Fig. 1) obtained using an $N = 130$-day-long averaging for the hydroacoustic stations CL (a) and DG (b). Each waveform was normalized by its maximum value. (c) Evolution of the peak signal-to-noise ratio $\mathrm{SNR}(L = 1, N)$ of the cross-correlation waveform between hydrophones 2 and 3 [see Eq. (4)] for increasing number N of averaging day ($N = 1$–130).

only) whose arrival time is close to L/c, where L is the separation distance of sensors 2–3 [see Fig. 1(a)] and c is a reference sound speed value of 1485 m/s typical for the SOFAR channel in the Indian Ocean (Chapp *et al.*, 2005). The clear temporal asymmetry of the averaged correlation waveforms $C_{\rm av}(t;\, L = 1,\, N = 130)$ confirms the dominant southern origin of the ocean background noise recorded by DG and CL stations in the frequency band (1–20 Hz) over the whole 130 day analysis period.

The peak signal-to-noise ratio (SNR) of each averaged cross-correlation waveform is defined as the ratio of the peak value of the main coherent arrival of $C_{\rm av}(t, L; N)$ [see Eq. (3)] to its standard deviation value at large time delays t where no coherent arrival is expected (selected here as the interval $1\,\mathrm{s} < |t| < 2\,\mathrm{s}$) (Sabra *et al.*, 2005a),

$$\mathrm{SNR}(L, N) = \frac{\max_t\{C_{\rm av}(t, L, N)\}}{\mathrm{std}\{C_{\rm av}(1\,\mathrm{s} < |t| < 2\,\mathrm{s}, L, N)\}}. \tag{4}$$

The standard deviation value is used here to estimate the level of residual temporal fluctuations of the cross-correlation waveform caused by the incoherent components of the noise field between hydrophones 2 and 3 (Sabra *et al.*, 2005a). Figure 2(c) compares the evolution of the signal-to-noise ratio $\mathrm{SNR}(L = 1, N)$ computed by averaging the cross-correlation waveforms across an increasing number of days N ($N = 1$–130) for both the DG array and the CL array. Note that the actual value of the SNR is directly related to the azimuthal directionality of the time-domain beamformer output displayed in Fig. 2. Theoretically, this SNR should increase as $\sqrt{N}$ in the presence of a stationary and diffuse noise field (Sabra *et al.*, 2005a; Weaver and Lobkis, 2005). However both experimental SNR curves appear to deviate from this theoretical prediction of $\sqrt{N}$ and display instead a stair-step pattern, especially for the CL array [see Fig. 2(c)]. This indicates that the directional coherent noise field emanating from Antarctica's coastline was highly non-stationary during the analysis period, most likely due to the physical generation mechanism of ice-breaking events.

To confirm this interpretation, Fig. 3 displays the amplitude variations of the intensity of the stacked averaged correlation waveform $C_{\rm av}(t, N, N + 15)$ [see Eq. (3)] for both CL and DG hydroacoustic stations using short moving average windows of 15 days, starting on a variable day N across the whole 130 day observation period ($1 \le N \le 115$). Furthermore, each stacked averaged cross-correlation waveform $C_{\rm av}(t, N, N + 15)$ was normalized by the value of its standard deviation for the same window $1\,\mathrm{s} < |t| < 2\,\mathrm{s}$ as previously used (i.e., $\mathrm{std}\{C_{\rm av}(1\,\mathrm{s} < |t| < 2\,\mathrm{s}, N, N + 15)\}$). Consequently, for a given value of N along the vertical axis, the maximum values displayed in Figs. 3(a) and 3(b) directly correspond to the peak signal-to-noise ratio SNR(N,N+15) [see Eq. (4)] of the corresponding correlation waveform $C_{\rm av}(t, N, N + 15)$ displayed here using a logarithmic scale. Overall, Fig. 3(a) [or Fig. 3(b)] shows that the peak SNR values vary widely between 20 and 45 dB (or 20 up and 40 dB) for

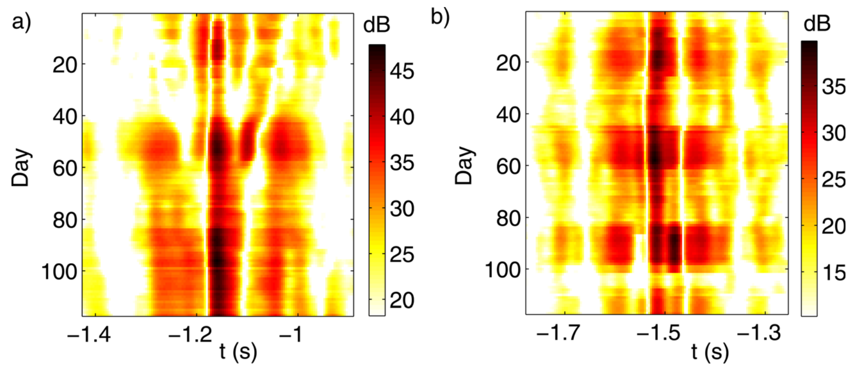

Fig. 3. (Color online) Amplitude variations (in logarithmic scale) of the intensity of the noise correlation waveforms $C_{av}(t, N, N+15)$ between hydrophones 2 and 3 (see Fig. 1) computed using short moving average windows of 15 days, starting on a variable day N across the whole 130 day observation period ($1 \leq N \leq 115$) for the hydroacoustic stations CL (a) and DG (b). Each correlation waveform $C_{av}(t, N, N+15)$ was normalized by the value of its standard deviation for the time-windows $1\,\mathrm{s} < |t| < 2\,\mathrm{s}$; such that the maximum displayed value—in logarithmic scale—on each day N effectively displays the peak signal-to-noise ratio SNR(N, N+15) [see Eq. (4)] of the corresponding correlation waveform $C_{av}(t, N, N+15)$. Note that each plot has a different color scale.

CL (or DG) station depending on which 15 day interval is selected, thus confirming the non-stationarity of the flux of coherent noise propagating between hydrophones 2 and 3 over the whole 130 day observation period.

4. Conclusions

The results presented in this letter indicate that coherent arrivals can be extracted from coherent processing of low-frequency noise (1–20 Hz) emanating from the vicinity of Antarctica's coastline. However, obtaining a consistent and relatively high SNR threshold (e.g., >20 dB) for the main coherent arrival of the noise cross correlation computed between a pair of hydrophones separated only by a short distance of $L = 2$ km requires at least several weeks of averaging. Assuming an ideal range and azimuth independent ocean as well as cylindrical spreading for these coherent arrivals propagating along the SOFAR channel, the coherent SNR [as defined in Eq. (4)] theoretically scales as a $\sqrt{T/L}$, where T denotes the total recording duration and L denotes the sensor separation distance (Roux *et al.*, 2004). Using this hypothetical scaling of the coherent SNR implies that achieving the same high SNR threshold value of 20 dB for a large sensor separation distance of $L = 1000$ km could require several years of averaging in the best case scenario! Hence, the possibility of extracting persistent coherent noise arrivals between the CL and DG hydroacoustic stations located across the whole Indian Ocean using only a few months long moving average window (e.g., to perform noise-based acoustic thermometry with a sufficient temporal resolution) does not seem feasible given the results presented in this letter.

Acknowledgments

Part of this work was supported by the Office of Naval Research. The authors would like to thank the reviewers for their detailed comments that helped improve the original manuscript.

References and links

Chapp, E., Bohnenstiehl, D. R., and Tolstoy, M. (**2005**). "Sound channel observations of ice-generated tremor in the Indian Ocean," Geochem., Geophys., Geosyst. **6**, Q06003.

DeGroot-Hedlin, C., and Orcutt, J. (**2001**). "Monitoring the Comprehensive Nuclear-Test-Ban Treaty: Hydroacoustics," Pure Appl. Geophys. **158**, 421–626.

Fried, S. E., Kuperman, W. A., Sabra, K. G., and Roux, P. (**2008**). "Extracting the local Green's function on a horizontal array from ambient ocean noise," J. Acoust. Soc. Am. **124**, EL183–188.
Gavrilov, A., and Li, B. (**2009**). "Correlation between ocean noise and changes in the environmental conditions in Antarctica," in *Proceedings of the 3rd International Conference and Exhibition on "Underwater Acoustic Measurements": Technologies and Results*, edited by J. S. Papadakis and L. Bjønø, Napflion, Greece, p. 1199.
Godin, O. A., Zabotin, N. A., and Goncharov, V. V. (**2010**). "Ocean tomography with acoustic daylight," Geophys. Res. Lett. **37**, L13605.
Leroy, C., Lani, S., Sabra, K. G., Hodgkiss, W. S., Kuperman, W. A., and Roux, P. (**2012**). "Enhancing the emergence rate of coherent wavefronts from ambient shipping noise correlations using spatio-temporal filters," J. Acoust. Soc. Am. **132**, 883–893.
Lin, F., Ritzwoller, M. H., and Shapiro, N. M. (**2006**). "Is ambient noise tomography across ocean basins possible," Geophys. Res. Lett. **33**, L14304.
Prior, M., Brown, D., and Haralabus, G. (**2011**). "Data features from long-term monitoring of ocean noise," in *Proceedings of the 4th International Conference and Exhibition on "Underwater Acoustic Measurements": Technologies and Results*, edited by J. S. Papadakis and L. Bjønø, Kos, Greece, p. 26.1.
Roux, P., Kuperman, W. A., and the NPAL Group (**2004**). "Extracting coherent wave fronts from acoustic ambient noise in the ocean," J. Acoust. Soc. Am. **116**, 1995–2003.
Sabra, K. G., Roux, P., and Kuperman, W. A. (**2005a**). "Emergence rate of the time-domain Green's function from the ambient noise cross-correlation function," J. Acoust. Soc. Am. **118**, 3524–3531.
Sabra, K. G., Roux, P., Thode, A., D'Spain, G. L., Hodgkiss, W. S., and Kuperman, W. A. (**2005b**). "Using ocean ambient noise for array element self-localization and self-synchronization," IEEE J. Ocean. Eng. **30**, 338–347.
Siderius, M., Song, H., Gerstoft, P., Hodgkiss, W. S., Hursky, P., and Harrison, C. (**2010**). "Adaptive passive fathometer processing," J. Acoust. Soc. Am. **127**, 2193–2200.
Weaver, R. L., and Lobkis, O. I. (**2005**). "Fluctuations in diffuse field-field correlations and the emergence of the Green's function in open systems," J. Acoust. Soc. Am. **117**, 3432–3439.
Westwood, E. K. (**1992**). "Broadband matched-field source localization," J. Acoust. Soc. Am. **91**, 2777–2789.